

# Amorphous multielementary alloys: A preparation route for shape memory alloys

P. Ochin<sup>a,\*</sup>, V. Kolomytsev<sup>b</sup>, A. Pasko<sup>b</sup>, A. Sezonenko<sup>b</sup>, Ph. Vermaut<sup>c</sup>, F. Prima<sup>c</sup>, R. Portier<sup>c</sup>

<sup>a</sup> CECM-CNRS, 15 rue G. Urbain, 94400 Vitry sur Seine, France

<sup>b</sup> Institute of Metal Physics NASU, 36 Verdnasky Bd, 03142 Kiev, Ukraine

<sup>c</sup> ENSCP, 11 rue P&M Curie, 75231 Paris Cédex 05, France

Available online 12 October 2006

## Abstract

Rapid solidification methods (planar flow casting and twin roll casting) have been used to improve and simplify processing of shape memory alloys. Our goal is to synthesize amorphous as-cast materials and then near-net shaping can be obtained while working in the supercooled liquid temperature region. Materials are thereafter crystallized in order to recover a reversible austenite–martensite transformation. Alloying equiatomic Ni–Ti intermetallic compound with selected elements leads to better glass forming ability (GFA). Despite the fact that compositional requirements for obtaining thermoelastic reversible martensitic transformation and glass formation are different and contradictory, the pseudo-binary alloys developed by substitution of Zr, Hf for Ti, and Cu, Co, Pd, Sn for Ni are good candidates to exhibit both phenomena. We report here a choice of compositions, which after fast cooling, are amorphous and demonstrate a superplastic behaviour in the  $\Delta T (T_x - T_g)$  region. After an adequate thermal treatment, a martensitic phase is obtained for some compositions, and such alloys demonstrate shape memory and superelastic properties. © 2006 Elsevier B.V. All rights reserved.

**Keywords:** Amorphous materials; Rapid solidification; Martensitic transformation; Shape memory

## 1. Introduction

Bulk metallic glasses (BMG) formers, on heating from the glassy state, shows a sharp viscosity drop in the undercooled liquid region just above  $T_g$  (glass transition temperature), with values changes from about  $10^{12}$  Pa s (typical for solids) to  $10^6$  Pa s. That can lead to an extremely large elongation (up to several thousands percent for specific compositions) by tensile deformation in the undercooled liquid region ( $T_x - T_g$ ), with  $T_x$  the crystallization peak temperature [1–3]. On the other hand, shape memory alloys (SMA's) are another class of materials finding an interest both from the academic and the industrial domains due to their unique functional properties, i.e. the one- and two-way shape memory effects (up to several percent of recoverable deformation), and the superelastic behaviour caused by a reversible martensitic transformation. The main condition for the obtaining of the SM effect is a thermoelastic equilibrium between the coexisting parent (austenite phase) and martensite phases and the formation of self-accommodated groups of

martensite crystals, having the same crystal structure but different orientations with highly mobile interfaces. Ni–Ti and Cu–Al based alloys remain the two major groups of commercially developed materials for industrial applications [4]. Meanwhile in many cases, especially for high temperatures applications (up to 200 °C and above), the SM applications are limited by the poor ductility of the currently available SMA [5]. To overcome the brittleness of binary alloys, one can modify the composition of the alloy by addition of elements in order to improve the mechanical behaviour and adjusting simultaneously the martensitic transformation temperature. Alternative production routes (direct shaping in forms close to end-users requirements) have been used, such as physical vapour deposition, powder metallurgy and rapid solidification processes. Very often in these methods, the material is received in the amorphous state. Then, an innovative technological path has been developed consisting in this scheme: multielementary alloy  $\Rightarrow$  melting + rapid solidification  $\Rightarrow$  amorphous phase = *metallic glass precursor of SMA*  $\Rightarrow$  shaping in the ( $T_x - T_g$ ) temperature range: *application of superplastic property*  $\Rightarrow$  crystallization stage  $\Rightarrow$  final microcrystalline material exhibiting a martensitic transformation in a predetermined temperature range. The new approach of metallic glass precursors, developed several years ago by Zhang et al.

\* Corresponding author. Fax: +33 1 46 75 04 33.

E-mail address: patrick.ochin@cecm.cnrs.fr (P. Ochin).

Table 1

Thermal properties of multielementary alloys (composition at.% according to the substitution rules A (Ti, Hf, Zr):B (Ni, Cu, Co, Pd, Ag, Sn) reported in this article (A = amorphous, C = crystalline phase))

	Chemical composition (at.%)	A:B	$T_q$ (°C)	XRD	$T_g$ (°C)	$T_x$ (°C)	$T_p$ (°C)	$\Delta T$ (°C)
1	Ti <sub>32</sub> Hf <sub>18</sub> Ni <sub>45</sub> Cu <sub>5</sub>	50:50	1300	A + C	465	505	507	40
2	Ti <sub>32</sub> Hf <sub>18</sub> Ni <sub>35</sub> Cu <sub>15</sub>	50:50	1290	A	449	493	496	45
3	Ti <sub>47</sub> Hf <sub>3</sub> Ni <sub>23</sub> Cu <sub>24.5</sub> Pd <sub>2</sub> Ag <sub>0.5</sub>	50:50	1320	A + C	433	474	479	41
4	Ti <sub>48</sub> Zr <sub>7</sub> Ni <sub>18</sub> Cu <sub>25</sub> Co <sub>2</sub>	55:45	1280	A	417	450	458	33
5	Ti <sub>27</sub> Zr <sub>18</sub> Ni <sub>40</sub> Cu <sub>15</sub>	45:55	1230	A	486	526	529	40
6	Ti <sub>40</sub> Hf <sub>18</sub> Ni <sub>40</sub> Cu <sub>15</sub>	55:45	1100	A	368	422	434	54
7	Ti <sub>45</sub> Zr <sub>5</sub> Ni <sub>20</sub> Cu <sub>25</sub> Sn <sub>5</sub>	50:50	1100	A	427	480	484	53

[6], have been successfully applied to the development of multi-components SMA systems [7,8]. We have noticed that the main alloyed elements are often the same for good BMG formers and good SMA.

From topological point of view, the increase in the degree of dense random packed structure is reflected in the difference of the atomic size distribution plots (ASDP) for “ordinary” amorphous phases and BMG’s. For a multielementary pseudo-binary AB alloy with appropriate ASPD, the largest GFA range should fit to the requirements for SMA, namely a “deep eutectic transition” near Ni<sub>50</sub>Ti<sub>50</sub> (at.%) for Ti–Ni based alloys or near to A<sub>75</sub>B<sub>25</sub> for Cu–Al and Ni–Al based alloys.

Concerning model alloys such as (Ti, Zr, Hf)A:(Co, Ni, Cu, Pd)B, the general requirements for SM composition and microstructure (to demonstrate high functional properties) may be summarized as follows: precise alloy composition (0.5–1 at.% maximum deviation); ordered parent phase (B2, DO<sub>3</sub>, or L2<sub>1</sub>), optimal grain size and 90% volume fraction of parent phase; reversible thermoelastic martensitic transformation which involves coherent and mobile parent phase–martensite phase boundaries; relatively narrow martensitic transformation hysteresis.

The challenging problem is to find a narrow chemical composition window, with respect to the established empirical rules for high amorphization ability [1,9], and restoration of the martensitic transformation and SM effects after crystallization. Detailed selection rules have been reported by Kolomytsev et al. [10].

In this paper we report a choice of examples of multicomponents pseudo-binary AB type (ratio A–B varied as 50:50, 55:45, 45:55) intermetallic compounds presented in Table 1. The reference multielementary alloys of the A:B type (Ni<sub>50</sub>Ti<sub>50</sub>) are formed with “A” = (Ti, Zr, Hf) and “B” = (Ni, Co, Cu, Pd, Sn). Substitution of Zr and Hf instead of Ti uses to increase the martensite transformation temperature. Co, Cu, Pd, Sn have been currently substituted to Ni for BMG forming.

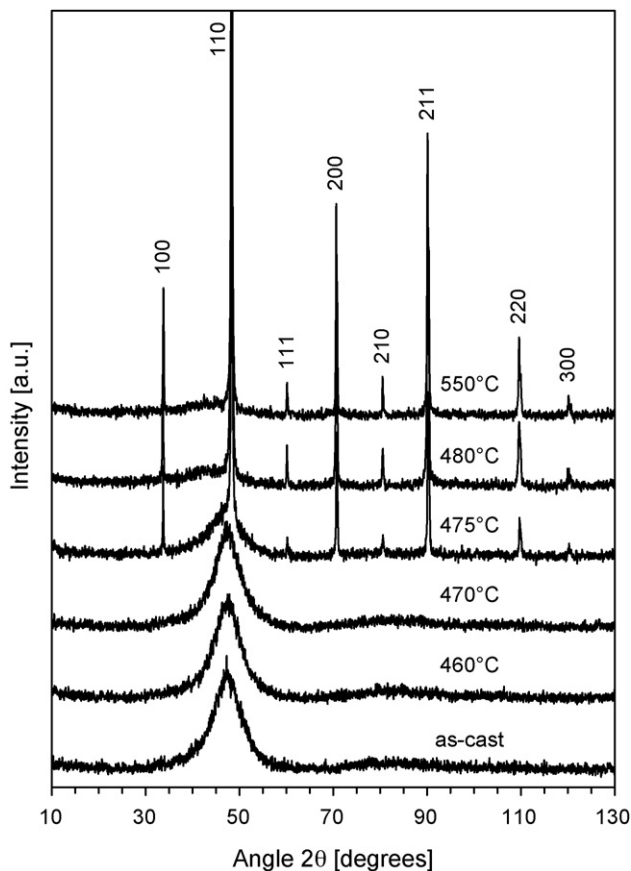


Fig. 1. XRD spectra of ribbon no. 2 Ti<sub>32</sub>Hf<sub>18</sub>Ni<sub>35</sub>Cu<sub>15</sub> in the as-cast state and after thermal treatment for 10 min at different temperatures: crystallization of amorphous phase into B2(CsCl).

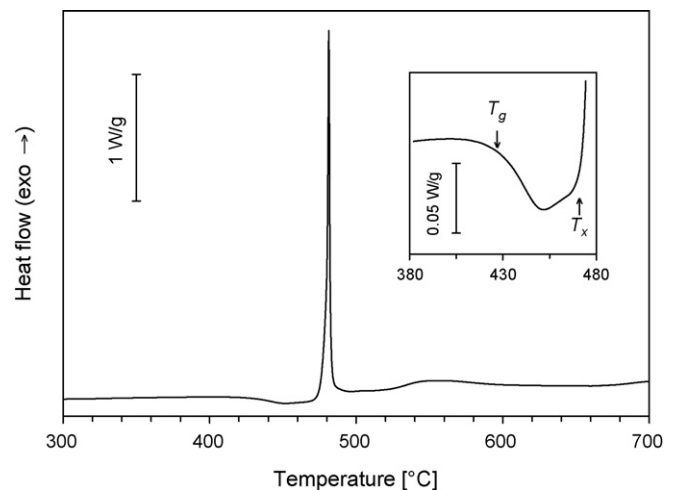


Fig. 2. DSC trace of as-cast Ti<sub>45</sub>Zr<sub>5</sub>Ni<sub>20</sub>Cu<sub>25</sub>Sn<sub>5</sub> (no. 7) ribbon (heating rate 10 K/min) showing the glass transition and crystallization of the amorphous phase.

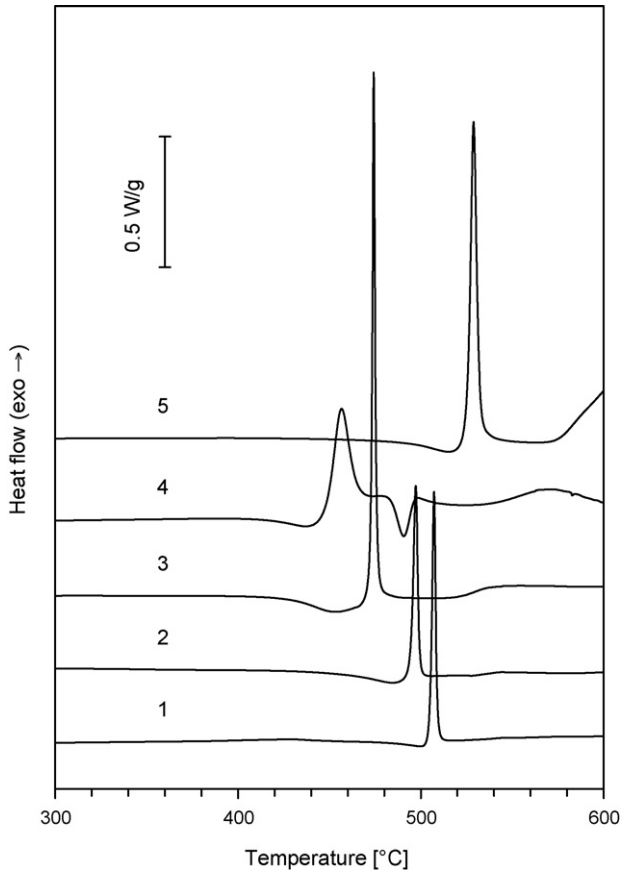


Fig. 3. Thermal analysis DSC of as-cast ribbons (10 K/min), sample nos. 1–5 (the origin of coordinates for various curves is shifted with respect to each other).

## 2. Experimental and results

The alloys have been prepared from pure commercial elements by induction melting in an inductive water cooled copper crucible and cast in a cooled copper cylindrical  $\varnothing$  12 mm mould. Thereafter ingots have been re-melted in quartz nozzles prior to be rapidly solidified on a spinning copper based wheel, using the planar flow casting method. Ribbons, average thickness 30  $\mu$ m, have been prepared at 20 m/s linear speed, 200 hPa ejection pressure, under a 1 bar He atmosphere as process parameters. Melt temperatures were chosen 100–150 K above liquidus temperatures according to the melt viscosity.

Experimental investigation namely X-ray diffraction, differential scanning calorimetry (DSC), mechanical testing in traction and optical microscopy observations have been performed for the alloys referenced in Table 1.

Most of as-cast ribbons are fully amorphous (broad halo peaks), others form a mixture of B2 austenite or B19 martensite crystals in an amorphous matrix (Table 1). After crystallization, B2 (austenite) or a mixture of B2 and B19 martensitic has been identified by XRD (Fig. 1).

As-received ribbons demonstrate, during DSC measurements on heating from room temperature, the classical behaviour of a metallic glass: i.e. a broad region of exothermic relaxation, an endothermic glass transition  $T_g$ , followed by one or several exothermic peaks ( $T_{x1}$ ,  $T_{x2}$ ) corresponding to successive trans-

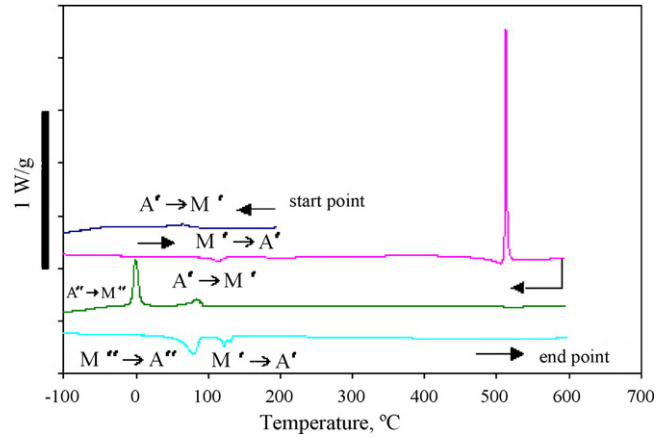


Fig. 4. DSC analysis of  $\text{Ti}_{32}\text{Hf}_{18}\text{Ni}_{45}\text{Cu}_5$  (no. 1) as-cast ribbon on cooling and heating two cycles (10 K/min). The martensitic transformation of a primary austenite  $A'$  is detected in the as-cast state. The crystallization process generates a secondary austenite  $A''$ .

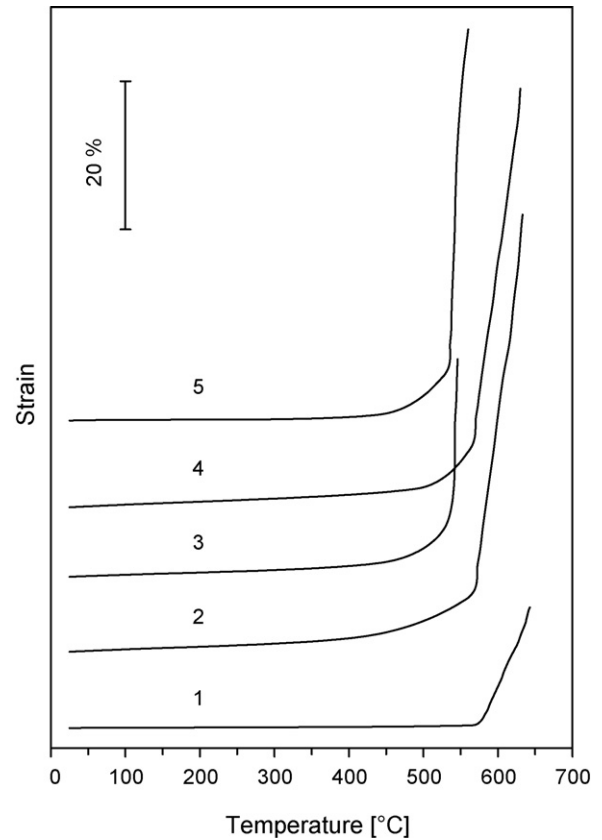


Fig. 5. Typical deformation in temperature demonstrating the superplastic behaviour of sample nos. 1–5 (the origin of coordinates for various curves is shifted with respect to each other along the strain axis).

Table 2  
Mechanical characteristics at room temperature of as-cast ribbons (Young's modulus and maximum strain recalculated from effective values taking into account the rigidity of the testing machine)

Sample reference	Composition (at.%)	Structure as-cast	Fracture strength (MPa)	Young's modulus (GPa)	Maximum strain (%)
1	$\text{Ti}_{32}\text{Hf}_{18}\text{Ni}_{45}\text{Cu}_5$	A + B2 + B19	684	76.1	0.89
2	$\text{Ti}_{32}\text{Hf}_{18}\text{Ni}_{35}\text{Cu}_{15}$	A	744	75.6	0.98
6	$\text{Ti}_{40}\text{Hf}_{15}\text{Ni}_8\text{Cu}_{37}$	A	1460	98.7	1.48

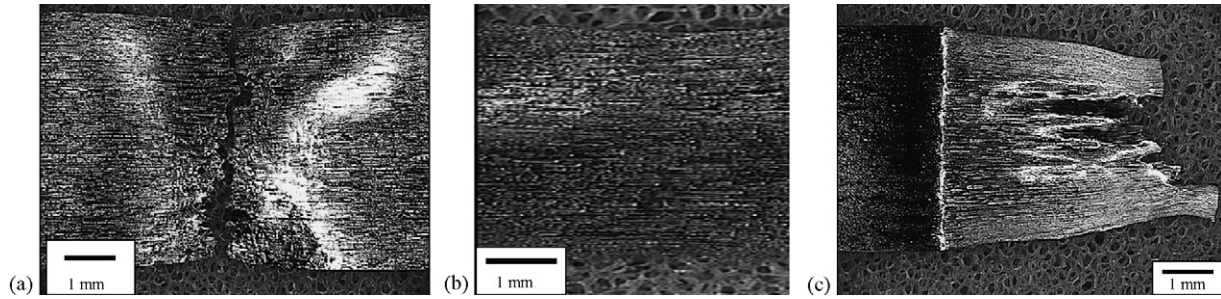


Fig. 6. Optical microscope pictures for ribbons nos. 1(a), 2(b) and 5(c) after “dynamic constant load”.

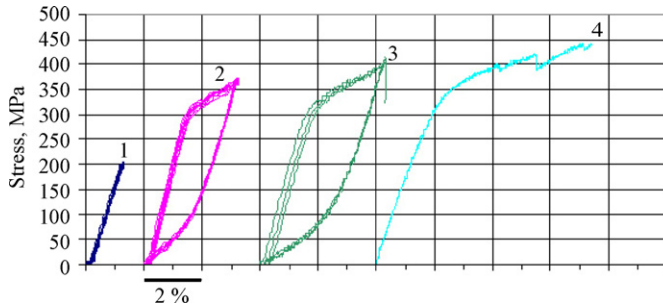


Fig. 7. Superelastic deformation property of ribbon no. 2 at room temperature after thermal treatment 900 °C, 1 h; the calorimetric final reverse martensite transformation temperature is  $A_F = +13$  °C (the origin of coordinates for various curves is shifted with respect to each other along the strain axis at repeated the loading/unloading cycles 1–4).

formations from the metastable liquid state to crystalline phases at different temperatures (Fig. 2).  $T_g$ , and  $T_x$  have been well identified for every alloy and the undercooled region measured (Table 1). A comparison of DSC thermal analysis between each composition is presented in Fig. 3 and values reported in Table 1. An example of typical thermal cycling is presented in Fig. 4, from the as-cast amorphous to the fully crystallized state in two successive phases. In Figs. 3 and 4, the origin of coordinates for various curves is shifted with respect to each other for better view. Generally, partially amorphous ribbons lead to two steps martensitic transformation after the crystallization process. This is due to two different natures and different microstructure of the austenite. One can distinguish a primary austenite  $A'$  crystallized directly from the melt during the rapid casting process, and a secondary austenite  $A''$  coming from the crystallization of the amorphous phase after heating above  $T_x$ . On the DSC curve Fig. 4, the  $A''$  transforms at lower temperature than  $A'$  probably because of a smaller grain size.

Mechanical tensile tests at room temperatures have been carried out on as-cast ribbons. Some mechanical characteristics are reported in Table 2 for quaternary (Ti, Hf)(Ni, Cu) ribbons A:B 50:50 nos. 1–2 and 55:45 no. 6. The superplasticity effect in the undercooled temperature region has been investigated with the dynamic constant load experiment, i.e. the deformation behaviour under constant load on heating from room temperature up to crystallization temperature  $T_x$  and above. For this purpose a stress of about 400 MPa (approximately 40–60% of the fracture stress value for the ribbons) was applied to the ribbon, and heating has been carried out at about 20 K/s, while keeping the same value of stress. Results are presented in Fig. 5 (the start point of various curves is shifted along the strain axis). A deformation of about 70% has been reached for fully amorphous ribbons and 20–30% for partially crystallized samples. Optical micrographs of selected ribbons with the highest  $\Delta T$ , are presented in Fig. 6 during tensile tests while increasing the temperature above  $T_g$ , one can notice the absence of large porosity developed in the deformed zone, which is significant of a viscous flow regime during deformation.

After crystallization at appropriate temperature, the superelastic property has been examined. The superelastic deformation scheme at room temperature

includes the tension up to some fixed chosen strain (2%, 3%, and more, up to the fracture) for a number of loading/unloading cycles. Cycling (stress versus deformation) is reported in Fig. 7 for the ribbon no. 2, for increasing stress values (the start point of various curves is shifted along the strain axis). A recoverable deformation up to 3% has been obtained due to the formation and growth of martensite on loading and its disappearance on unloading.

### 3. Concluding remarks

A technological route has been developed for the production of shape memory alloys allowing an easier shaping, in the undercooled region, of corresponding amorphous precursors alloys. The chemical compositions of precursor alloys have been designed according to selection rules based on empirical rules for BMG and specific restrictions linked to the obtaining of a martensitic transformation from a high temperature austenite type phase. A series A:B type multielementary alloys (with  $A = \text{Ti, Hf, Zr}$  and  $B = \text{Ni, Cu, Co, Pd, Ag, Sn}$ ), has been prepared and rapidly solidified into metallic glasses or partially crystalline amorphous phases that demonstrate a superplastic deformation in the undercooled temperature zone. After adequate thermal treatments carried on as-cast materials, some of the multicomponent alloys demonstrate superelastic characteristics of SMA.

### References

- [1] A. Inoue, Mater. Trans. JIM 36 (1995) 866–875.
- [2] H.A. Bruck, T. Christman, A.J. Rosakis, W.L. Johnson, Scripta Metall. Mater. 30 (1994) 429–434.
- [3] T.A. Waniuk, J. Schroers, W.L. Johnson, Appl. Phys. Lett. 78 (1998) 3665–3667.
- [4] T.W. Duerig, K.N. Melton, D. Stoekel, C.M. Wayman, Engineering Aspects of Shape Memory Alloys, Butterworth and Heinemann, 1990.
- [5] G.S. Firstov, J. Van Humbeeck, Y. Koval, Mater. Sci. Eng. A 378 (2004) 2–10.
- [6] T. Zhang, A. Inoue, T. Masumoto, Mater. Sci. Eng. A 181–182 (1994) 1423–1426.
- [7] V. Kolomytsev, M. Babanly, R. Musienko, A. Sezonenko, P. Ochin, A. Dezellus, P. Plaindoux, F. Dalle, P. Vermaut, R. Portier, J. Phys. IV France 11 (2001), Pr8 475–480.
- [8] V. Kolomytsev, M. Babanly, R. Musienko, A. Sezonenko, P. Ochin, A. Dezellus, P. Plaindoux, P. Vermaut, R. Portier, J. Phys. IV France 11 (2001), Pr8 457–462.
- [9] A. Inoue, Acta Mater. 48 (2002) 279–306.
- [10] V. Kolomytsev, A. Pasko, A. Sezonenko, Arch. Metall. Mater. 49-4 (2004) 825–840.